Kinetics on Organic Removal by Aerobic Granular Sludge in Bubbled Airlift Continuous Reactor

Andik Yulianto*, Nida Maisa Zakiyya, Prayatni Soewondo, Marisa Handajani & Herto Dwi Ariesyady

Environmental Engineering Department, Faculty of Civil Engineering and Environmental, Institut Teknologi Bandung, Jalan Ganesha No.10 Bandung 40132, Indonesia
*E-mail: yulianto.andik@gmail.com

Abstract. An assessment of aerobic granular sludge (AGS) in a bubbled airlift continuous reactor (BACR) was done to determine the AGS growth kinetics in the continuous reactor and the impact of varied hydraulic retention time (HRT) against the AGS structure. Sodium acetate was used as the sole carbon source with a 100:20 ratio of COD/N synthetic water. The system was operated at five variations of HRT, i.e. 12, 10, 8, 6, and 4 hours, with organic loading rate (OLR) ranging from 1.6 to 4.8 g COD/day in the BACR. Organic removal decreased from 73% to 52%, along with the increment of OLR, while HRT decreased from 12 hours to 4 hours. The kinetics of organic removal in the BACR were examined to get a better understanding of organic removal trends by AGS in a BACR. The models used for biomass growth analysis were the Monod, Contois, Grau second-order, and Stover-Kincannon kinetic models. This study showed that the best suited models for organic removal in BACR were the Grau second-order kinetic model with an *a* value of 0.1382 and a *b* value of 1.0776, and the Stover-Kincannon kinetic model with an R_{max} of 5.8 g COD/L.day and a K_B of 6.24 g COD/L.day.

Keywords: *aerobic; aerobic granular sludge; bubbled airlift reactor; Contois; Grau second-order; Monod; Stover-Kincannon.*

1 Introduction

Conventional activated sludge systems have been widely implemented for over decades, but they have some drawbacks: high generated biomass volume, fluctuating loading rates, and large required area [1]. Aerobic granular sludge (AGS) is a promising novel technology for the treatment of biological wastewater. It consists of biofilm particles formed by complex microbial self-aggregation under very specific conditions. Some notable advantages of AGS have been reported: excellent settleability, compact microbial structure, high biomass retention, high organic loading resistance, and tolerance to toxicity [2,3]. Moreover, compared to conventional activated sludge, AGS has a smoother surface, a faster start-up time, shorter settling time and longer

Received February 2nd, 2019, 1st Revision April 22nd, 2019, 2nd Revision June 10th, 2019, Accepted for publication August 20th, 2019.
 ISSN: 2337-5779, DOI: 10.5614/j.eng.technol.sci.2019.51.5.7

retention time [4]. This may be explained by the low sludge volume index (SVI) of AGS (in the range of 50-85 mL/g), which is lower than activated sludge (usually 150 mL/g of SVI) [5-7]. AGS formation in a sequencing batch reactor (SBR) has already been proved to support a good physical structure of the granules and high organic removal efficiency. Formation of AGS in a sequencing batch reactor (SBR) has also been studied and proved to support a good physical structure of the granules and high removal efficiency in treating wastewater, especially for organic and nutrient removal. It is formed in five phases of the batch process: the filling, aeration, settling, decanting, and idle phases [3,8]. Granulation of AGS in a full-scale SBR has been conducted in China [9], resulting in a more compact structure and excellent settling ability compared to sludge produced in anaerobic/anoxic plug flow and oxidation ditch reactors. The SBR operating cycle with feast-famine period, shorter settling time, and no-return sludge pump is considered to play an important role in the granulation process. However, issues related to SBR operation have been raised for large-scale operation, especially in the decanting mechanism, skimming, and floatable materials. Furthermore, several key factors need to be fulfilled to maintain the SBR process and operation, including process equipment, monitoring and operational procedures, and adequate training of manpower [10]. On the other hand, a continuous operating system provides significant key features that the SBR system does not provide. It is considered to be more stable in operation, has less risk of BOD fluctuation, and is easier to maintain and monitor [10].

This study conducted continuous operation for organic removal by AGS using a bubbled airlift continuous reactor (BACR). BACRs are known to deliver good hydrodynamics performance and maintain the homogeneity of the shear force in the reactor, which is suitable to maintain the AGS structure [11,12]. The inner circulation of the liquid in the airlift reactor is suspected to be the primary contributor to the aerobic granulation process [13]. Removal kinetics were determined to get a better understanding of the organic removal trends by AGS in a BACR. The organic matter kinetics in the SBR reactor were investigated and assessed to know the limitations of substrate mass transfer of organic matter into the granules [14], which can also be classified as biosorption [15,16]. This research focused on organic removal kinetics in a BACR by observing substrate fluctuation during various operational HRTs.

2 Methods

2.1 Seeding

Seeding was carried out using a 10-liter container for 2 weeks, using sucrose as the primary substrate with the addition of nutrients. Acclimatization occurred indirectly due to the sludge's adaptation to the sucrose as the sole carbon substrate. Aeration was run during seeding until it reached 2000 mg/L of mixed liquor suspended solids (MLSS). Two parameters, i.e. pH and DO, were also monitored. pH was maintained in the range of 6-8, while DO was supplied via aeration to keep it at around 7 mg/L.

2.2 Granulation

AGS was cultivated in previous study [17]. AGS was first cultivated in an SBR column with a height of 1.2 m, a diameter of 0.05 m, and a volume of 2.4 L. It was conducted in an 8-hour operational cycle, as recommended by Liu [18], with 60 minutes of filling, 407 minutes of aeration, 5 minutes of settling, and 8 minutes of decanting. Granulation was set for 20 days of operation with an OLR of 2.5 kg/COD/day as this has been proved as the optimum OLR for granulation [19,17,20] and 3 L/minute of aeration from the bottom of the SBR to provide 2.55 cm/s of superficial velocity.

2.3 Reactor Set Up

The BACR was seeded with AGS produced from the SBR with an OLR of 2.5 kg/COD/day and tested with five HRT variations to see the kinetic process in the continuous system. The BACR, adapted from Zhou, *et al.* [12], consisted of two coaxial cylinders, with the outer diameter of 8 cm, the inner diameter of 5 cm, and a height of 1.4 m, resulting in 7 L of working volume of the reactor. Synthetic wastewater was fed and fine air bubbles were pumped from the bottom of the reactor to supply aeration and provide 2.55 cm/s of superficial velocity (see Figure 1).

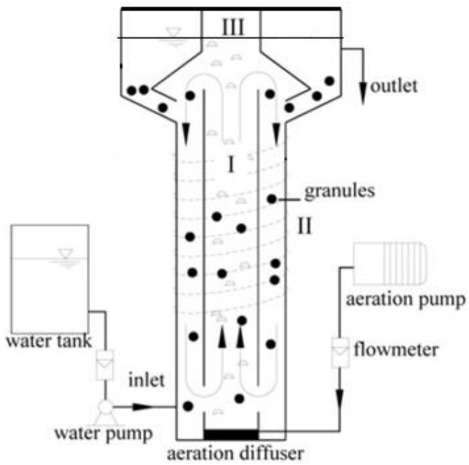

Figure 1 Bubbled airlift continuous reactor (BACR).

Operation was started with 12 hours of HRT, then decreased to 10 hours of HRT, 8, 6, and finally 4 hours of HRT. Each of the running conditions took 2 days of operational time. This operational time was considered by doing a test to check the organic concentration and organic removal as main criteria for steady state condition.

2.4 Synthetic Water

Sodium acetate was chosen as source of organic carbon due to its simple chemical structure. NH_4Cl, K_2HPO_4, and KH_2PO_4 were used as sources of nitrogen and phosphorus. Microelements incorporated in the system were $CaCl_2.2H_2O$ and $MgSO_4.7H_2O$. The composition of synthetic wastewater was adapted from Koh [19], as listed in Table 1.

Table 1 Composition of synthetic wastewater.

Material	Concentration
$NaCH_3COOH$	3110.8 mg/L
NH_4Cl	764.3 mg/L
K_2HPO_4	28.1 mg/L
KH_2PO_4	22 mg/L
$CaCl_2.H_2O$	37.5 mg/L
$MgSO_4.7H_2O$	31.3 mg/L

2.5 Analytical Methods

All parameters were analyzed according to the Standard Method for the Examination of Water and Wastewater (SMEWW) (Table 2). The settling velocity was determined by dividing the distance of the settling test with the settling time. The granule diameter was measured using microscopic view of an Olympus Microscope CX31RTSF, Japan, and measured according to the magnification used.

Table 2 Parameters and analytical methods.

Parameter	Sampling period	Methods
pH	8 hours	SMEWW 4500 H+
Temperature	8 hours	SMEWW 2550
DO	8 hours	SMEWW 4500-O
COD	8 hours	SMEWW 5220C
MLSS	8 hours	SMEWW 2540-D
SVI	Before and after operation	SMEWW 2710-D
Settling velocity	Before and after operation	SMEWW 2710-E
Size of the granule	1 day	*
Granule structure	Before and after operation	SMEWW 9211-B

* Determined by direct observation of the AGS

2.6 Data Analysis

Four models were used in this research: the Monod, Contois, Grau second-order, and Stover-Kincannon kinetic models. The equations (Eqs. (1) to (11)) of each model are briefly described in Table 3 [21]. The Monod kinetic model assumes that the half-saturation constant (Ks) is independent from the population density, whereas the Contois kinetic model assumes that Ks are dependent on the population density [22]. The Stover-Kincannon kinetic model assumes that the substrate utilization is affected by OLR [23], and the Grau second-order model was derived from combining the Monod model and the kinetics of the chemical reaction, which simulates gradual diminution of individual components with time and is not limited to integers only [24].

Table 3 Kinetic equations.

Kinetics	Equations	
Monod	$\frac{So-S}{\theta_H X} = \frac{1}{Y\theta_c} + \frac{Kd}{Y}$	(1)
	$\frac{\theta_c}{1+\theta_c Kd} = \frac{Ks}{\mu_{maks}}\frac{1}{S} + \frac{1}{\mu_{maks}}$	(2)
	$S = \frac{Ks(1+Kd\theta_c)}{\mu_{maks}\theta_c - Kd\theta_c - 1}$	(3)
Contois	$\frac{\mu_{maks} S}{\beta X+S} = \frac{1}{\theta_c} + Kd$	(4)
	$\frac{\theta_c}{1+\theta_c Kd} = \frac{\beta}{\mu_{maks}}\frac{X}{S} + \frac{1}{\mu_{maks}}$	(5)
	$S = \frac{\beta X(1+Kd\theta_c)}{\mu_{maks}\theta_c - Kd\theta_c - 1}$	(6)
Grau second-order	$\frac{So\theta_H}{So-S} = \theta_H + \frac{So}{k_s X}$	(7)
	$\frac{So\theta_H}{So-S} = a + b\theta_H$	(8)
	$S = So\left(1 - \frac{\theta_H}{a+b\theta_H}\right)$	(9)
Stover-Kincannon	$\frac{V}{Q}(So - S) = \frac{K_B}{R_{maks}}\left(\frac{V}{QSo}\right) + \frac{1}{R_{maks}}$	(10)
	$S = So - \frac{R_{maks}So}{K_B + (QSo/V)}$	(11)

3 Results

3.1 Granule Characterization

The AGS was taken from the granule cultivation in previous study [17]. It was formed in an SBR for three weeks, resulting in approximately AGS with a size of 2 mm size and 55.714 mL/g of SVI, 2100 mg/L of MLSS, an aspect ratio of 0.8, and a removal capacity of 79% for 300 mg/L of initial COD.

3.2 Effect of HRT on AGS Structure

Investigation of the removal of organic substrates using AGS was done in a BACR with 5 HRT variations in 10 days in total. Continuous operation was started with 12 hours of HRT until COD removal reached steady state. The HRT was gradually decreased every 2 days, to 10, 8, 6, and 4 hours. This section explains the granule's structural characteristics, specifically diameter, settling velocity, and SVI. In continuous operation, it was found that diameter and settling velocity slowly decreased over time. The granule diameter decreased to 0.6 mm while the settling velocity of AGS decreased up to 7.9 m/hour and the SVI increased from 58.4 mL/g on day 0 to 120 mL/g on day 10 (Figures 2 and 3).

Diameter, settling velocity, and SVI were considered as the main parameters in order to classify the strength of the AGS [25]. Tay, *et al.* [26] state that the SVI of AGS is about 50 to 80 mL/g. As can be seen in Figure 5, the SVI was above 80 mL/g after the 4th day.

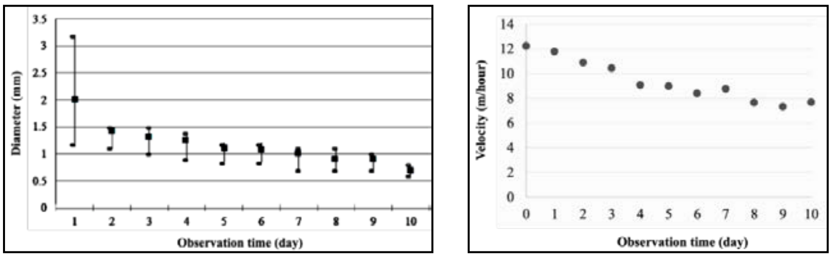

(a) (b)

Figure 2 Changes in (a) granular diameter and (b) settling velocity per day.

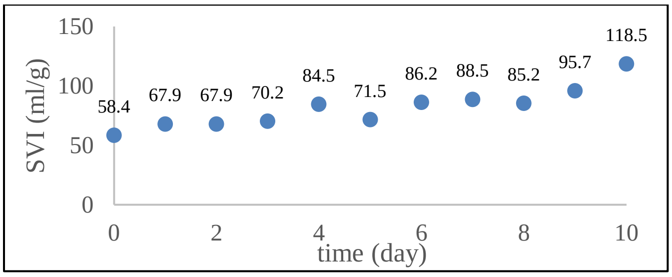

Figure 3 Changes in SVI during operation.

Further microscopic observation was used to observe the granule morphology. From microscopic observation, the granule surface was clear with no filamentous bacteria existing since the beginning of continuous operation. Its shape was almost completely round and solid, but after the 4th day, the AGS was starting to deteriorate, as can be seen in Figure 4. This condition occured while the reactor operation entered the third phase with 8 hours of HRT. This AGS breakage lead to a decrease in diameter and settling velocity, and an increase of the SVI.

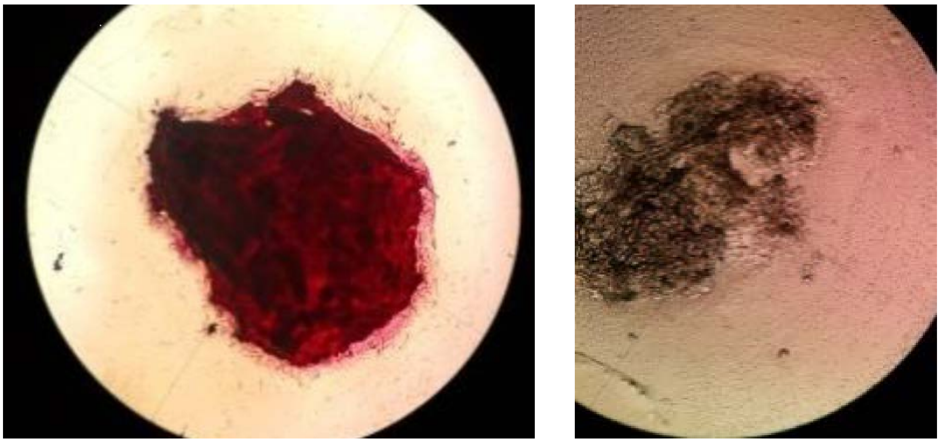

(a) (b)

Figure 4 (a) Initial condition with 40x magnification (day 1), and (b) broken granule structure with 40x magnification (day 4, entering day 5).

3.3 Effect of HRT on the Organic Removal and Biomass

The experiment consisted of 5 HRT variations that gradually decreased every 2 days to ensure its steady state condition: 12, 10, 8, 6, and 4 hours of HRT. In the 12 hours of HRT, organic removal reached 73%. As HRT decreased to 10 hours, organic removal also decreased to 70%. COD removal in steady state condition continuously decreased in every HRT variation conducted. It ended with 52.4% COD removal efficiency at 4 hours of HRT.

From Figure 5 it can be concluded that the increase of organic removal was directly proportional to HRT, with a slope of 0.0265 and an R^2 of 0.8935. Similarly, the biomass concentration in the reactor was also directly proportional to HRT with a slope of 0.0928 and an R^2 of 0.8299. The decreased amount of MLSS at a short retention time caused the biomass to be washed out. This also happened in a previous study, where washout occurred in a completely stirred tank reactor when the HRT was decreased to 2.4 hours [27].

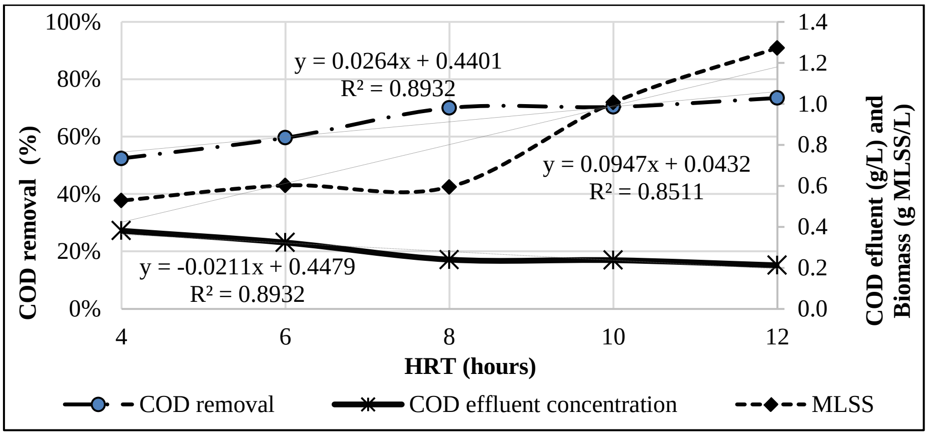

Figure 5 The effect of HRT on MLSS and organic removal efficiency.

Figure 6 shows the decrease in substrate removal efficiency during operation, leaving a steady concentration of effluent substrate in each phase. Washed-out suspended solid may indicate AGS disintegration and affect retention rate reduction [28]. AGS can be broken because of several conditions, such as AGS mass transfer limitation when AGS formation reaches a large granule diameter [29]. Dead bacteria inside the granules may also weaken the granule structure, eventually leading to disintegration [25].

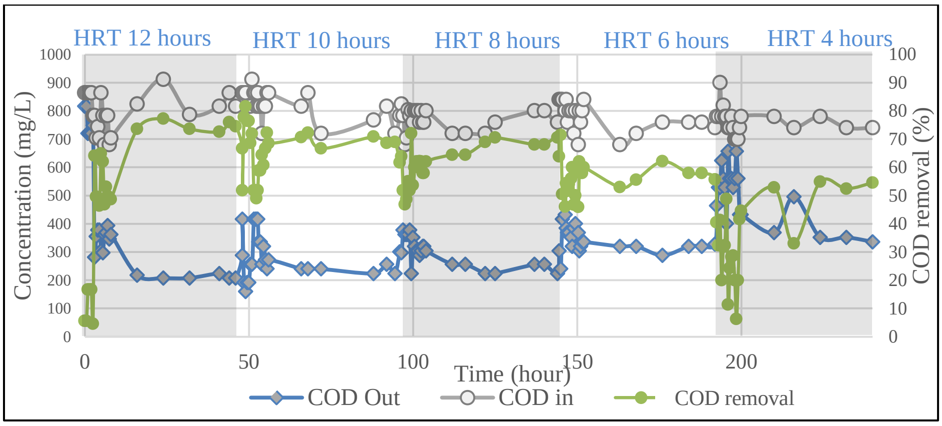

Figure 6 Comparison of COD concentration at the inlet and outlet, and the percentage of COD removal.

OLR also has an effect on the system. Once the OLR gets too high, it could lead the AGS to be ruptured and deteriorated. Val del Rio, *et al.* [28] stated that the maximum acceptable OLR to maintain the AGS structure is 4.4 kg COD/m3/day.

As for this study, a decrease of HRT resulted in an increased OLR ranging from 1.6 to 4.8 g COD/day. The experiment showed that the AGS disintegrated at an HRT of 8 hours (for OLR higher than 3.2 g COD/day). The running sequence of HRT variations may also have played a role in this, considering that AGS activities could be affected by several different operating systems through OLR increment. Therefore a parallel operation system is suggested for further research in order to confirm the influence of the operating system.

3.4 Kinetic Models

The kinetic parameters of the Monod model can be determined using Eqs. (6) and (7), as shown in Figure 7. From Figure 7(a), Y and Kd are 1.62 and 0.59 day^{-1}, while from Figure 7(b), μmax and Ks are 1.16 day^{-1} and 0.51 g COD/L.

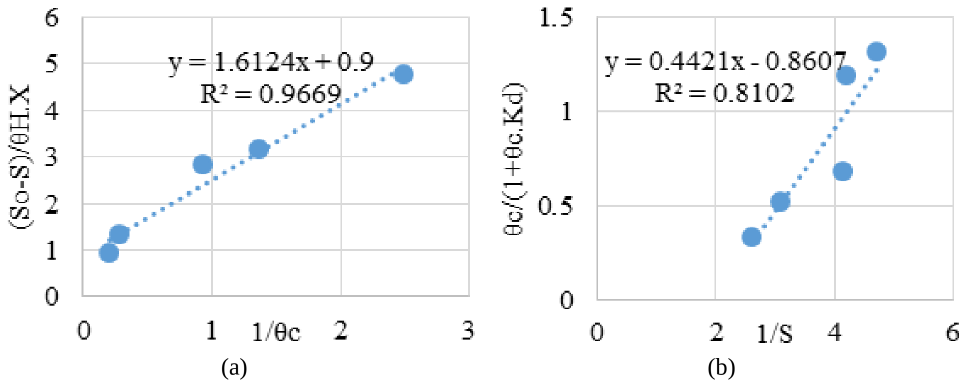

Figure 7 Monod kinetic model: (a) the relationship (So-S)/θH with θc, and (b) the relationship θc/(1 + θc.Kd) by 1/S.

By regression $\theta_c/(1 + \theta_c.Kd)$ to *X/S*, the gradient and intercept of the line were obtained as 0.0465 and 0.1971. Thus, it can be seen that the kinetic parameters Contois μ_{max} and β were respectively 5.07 day^{-1} and 0.24 g COD/L. With the same method (see Figure 5), the kinetic parameters for the Grau second-order model resulted in a dimensionless Grau second-order constant *a* value of 0.1382 and a *b* value of 1.0776, and the Stover-Kincannon model gave a result of 5.8 g COD/L.day as maximum utilization constant (R_{max}) and 6.24 g COD/L.day for the saturation value constant (K_B) (see Figure 8).

To determine the best fit kinetic model, as adopted by Jijai [21], the organic removal kinetic was calculated under steady-state condition, where the AGS activity on organic degradation was already stable [21,22,30,31]. The predicted COD from the model equations was then compared with the measured COD.

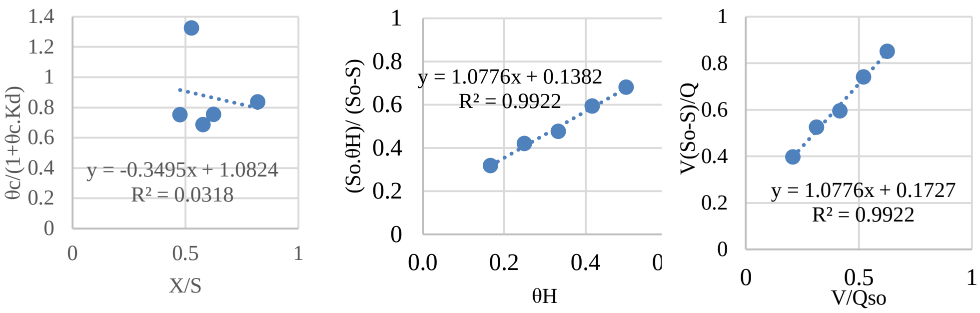

(a) (b) (c)

Figure 8 Linear regression of (a) Contois, (b) Grau second-order, (c) Stover-Kincannon kinetic model.

From the comparison shown in Figure 9, the Grau second-order and Stover-Kincannon model were the best fit models to represent the process of AGS activity in the system, with an R^2 of 0.957. The Stover-Kincannon kinetic model assumes that the substrate concentration at *t* time is dependent on OLR [23].

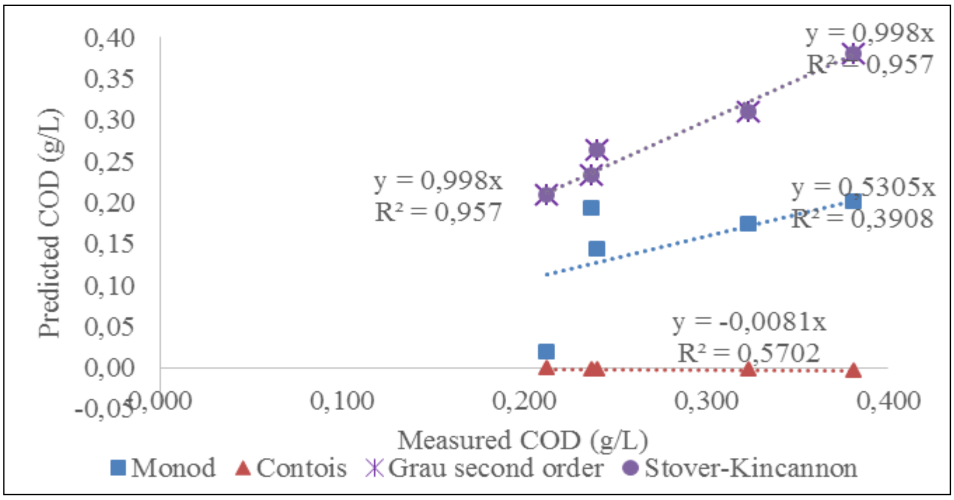

Figure 9 Comparison of measured COD and predicted COD.

In previous studies, the kinetic models were usually applied on a UASB reactor, resulting in *a* and *b* values for the Grau second-order as shown in Table 4. For the Stover-Kincannon model, the maximum utilization constant (R_{max}) and saturation value constant (K_B) in this study were lower than the values obtained for cassava wastewater using a UASB [21] and similar to other substrates from textile wastewater [30,31]. In this case, the BACR provided by aerobic system while the main operation was conducted continuously by anaerobic system. To improve AGS microbial activity some suggestions can be done to improve the quality of the AGS structure and increase the organic removal capacity by adjusting some technical parameters in BACR, including HRT.

Table 4 Kinetic parameter comparison.

Grau Second-order					
COD (mg/L)	**HRT (day)**	**OLR (kg COD/m^3.day)**	**a**	**b**	**Reference**
18800	1-5	3.76-18.8	0.40	1.01	[21]
18800	1-5	3.76-18.8	0.89	0.94	[21]
18800	1-5	3.76-18.8	2.15	0.97	[21]
4214	0.25-4.17	1.0-15.8	0.56	1.10	[30]
3000	0.083-0.83	6-34	0.03	0.01	[31]
800	0.167-0.5	1.6-4.8	0.14	1.08	This study
Modified Stover-Kincannon					
COD (mg/L)	**HRT (day)**	**OLR (kg COD/m^3.day)**	**K_B (g COD/L.day)**	**R_{max} (g COD/L.day)**	**Reference**
18800	1-5	3.76-18.8	48.24	47.62	[21]
18800	1-5	3.76-18.8	20.06	21.28	[21]
18800	1-5	3.76-18.8	6.11	8.77	[21]
4214	0.25-4.17	1.0-15.8	8.21	7.50	[30]
3000	0.083-0.83	6-34	0.03	0.01	[31]
800	0.167-0.5	1,6-4,8	6.24	5.79	This study

4 Conclusions

Four kinetics models were used to get the best fit model for representing AGS behavior in a BACR: the Monod, Contois, Grau second-order, and Stover-Kincannon kinetics models. The two best kinetic models to represent the relationship between the AGS and its substrate were the Grau second-order model with kinetic parameters *a* and *b* values of 0.1382 and 1.0776 respectively, and the Stover-Kincannon model with an R_{max} parameter value of 5.8 g COD/L.day and a K_B value of 6.24 g COD/L.day.

From this study it can be concluded that OLR affects the substrate utilization at different concentrations. However, this study still needs to be further developed since the AGS structures were still vulnerable and washout could occur. Some suggestions to be considered for future studies are: (1) improving the aerobic granular structure stability, (2) conducting each HRT variation using the initial sample within the same period of time to test the effect of HRT on the granules quality.

Acknowledgments

The authors would like to thank the Directorate of Research and Community Services, Ministry of Research, Technology and Higher Education, Indonesia and Institute for Research and Community Services (LPPM), Institut Teknologi Bandung for their funding support through the Research and Community Service Grant Scheme 2015-2016.

Nomenclature

X_o	=	initial concentration of biomass (mg/L)
X_e	=	effluent concentration of biomass (mg/L)
X	=	concentration of biomass in system (mg/L)
Q	=	flow rate of influent (L/day)
V	=	reactor volume (L)
μ	=	specific growth rate (day^{-1})
K_d	=	decay rate of the biomass (day^{-1})
θ_c	=	sludge retention time (SRT) (day)
μ_{max}	=	maximum specific growth rate (mg/L)
S	=	substrate concentration (mg/L)
K_s	=	half-saturation constant (g COD/L)
β	=	Contois kinetic coefficient (g COD/g biomass)
b	=	Grau second order constant (g/L)
K_B	=	saturation constant (g COD/L.day)
R_{max}	=	maximum utilization rate constant (g COD/L.day)

References

[1] Beun, J., van Loosdrecht, M. & Heijnen, J., *Aerobic Granulation in a Sequencing Batch Airlift Reactor*, Water Research, **36**, pp. 702-712, 2002.

[2] Adav, S., Lee, D.J., Show, K.Y. & Tay, J.H., *Aerobic Granular Sludge: Recent Advances*, Biotechnology Advances, **26**, pp. 411-423, 2008.

[3] Beun, J., Hendriks, A., van Loosdrecht, M., Morgenroth, E., Wilderer, P. & Heijnen, J., *Aerobic Granulation in a Sequencing Batch Reactor*, Water Research, **33**(10), pp. 2283-2290, 1999.

[4] Chen, Y., Jiang, W., Liang, D. & Tay, J., *Aerobic Granulation under the Combined Hydraulic and Loading Selection Pressure*, Biosource Technology, **99**, pp. 7444-7449, 2008.

[5] Tay, J., Tay, S., Show, K., Liu, Y. & Ivanov, V., *Aerobic Biomass Granules for Wastewater Treatment*, U.S. Patent No US 6,793,822 B2, US: U.S. Patent No US 6,793,822 B2, 2004.

[6] Liu, Q., Tay, J. & Liu, Y., *Substrate Concentration-Independent Aerobic Granulation in Sequential Aerobic Sludge Blanket Reactor*, Environmental Technology, **24**, pp. 1235-1243, 2003.

[7] Qin, L., Tay, J. & Liu, Y., *Selection Pressure is a Driving Force of Aerobic Granulation in Sequencing Batch Reactors,* Process Biochemical, **39**, pp. 579-584, 2004.

[8] Wagner, J. & da Costa, R., *Aerobic Granulation in a Sequencing Batch Reactor Using Real Domestic Wastewater*, Journal of Environmental Engineering, **139**, pp. 1391-1396, 2013.

[9] Li, J., Ding, L.B., Cai, A., Huang, G.X. & Horn, H., *Aerobic Sludge Granulation in a Full-Scale Sequencing Batch Reactor*, BioMed Research International, Article ID 268789, 12p., 2014.

[10] Silva, V. de, *Operating SBR Plants-Issues and Concerns*, Water Environment Federation, January 2003.

[11] Tijhuis, L., Loosdrecht, M. van & Heijnen, J., *Formation and Growth of Heterotrophic Aerobic Biofilms on Small Suspended Particles in Airlift Reactors,* Biotechnology and Bioengineering, **44**, pp. 595-608, 1994.

[12] Zhou, D., Liu, M., Wang, J., Dong, S., Cui, N. & Gao, L., *Granulation of Activated Sludge in a Continuous Flow Airlift Reactor by Strong Drag Force*, Biotechnology and Bioprocess Engineering, **18**, pp. 289-299, 2013.

[13] Wan, J.F., Mozo, I., Filali, A., Line, A., Bessiere, Y. & Sperandio, M., *Evolution of Bioaggregate Strength during Aerobic Granular Sludge Formation*, Biochem Eng, **58-59**, pp. 69-78, 2011.

[14] Liu, Y., Liu, Y. & Tay, J., *Relationship Between Size and Mass Transfer Resistance in Aerobic Granules*, Letters in Applied Microbiology, **40**, pp. 312-315, 2005.

[15] Fulazzaky, M.A., Nuid, M., Aris, A. & Muda, K., *Kinetics and Mass Transfer Studies on the Biosorption of Organic Matter from Palm Oil Mill Effuent by Aerobic Granules before and after the Addition of Serratia marcescens SA30 in a Sequencing Batch Reactor*, Process Safety and Environmental Protection, **107**, pp. 259-268, 2017.

[16] Fulazzaky, M.A., Nuid, M., Aris, A. & Muda, K., *Mass Transfer Kinetics of Biosorption of Nitrogenous Matter from Palm Oil Mill Effluent by Aerobic Granules in Sequencing Batch Reactor*, Environmental Technology, **39**, pp. 2151-2161, 2018.

[17] Putri, K., *Determination of Optimum C/N Ratio for Aerobic Granules in Sequencing Batch Reactor*, Master Thesis, Bandung, Indonesia: Institut Teknologi Bandung, 2016. (Text in Indonesian)

[18] Liu, Y. & Tay, J., *State of The Art of Biogranulation Technology to Wastewater Treatment*, Biotechnology Advances, **22**, pp. 533-563, 2004.

[19] Koh, K., Kueh, K., Loh, K.T., Leong, H., Chu, A.S. & Hashim, M., *Effect of Seeding Sludge Type and Hydrodynamic Shear Force on the Aerobic Sludge Granulation in Sequencing Batch Airlift Reactor*, J. Chem. Eng, **4**, pp. 826-831, 2009.

[20] Pertiwi, M., *Effect of Settling Time and Substrate Type on Granulation with Sequencing Batch Reactor,* Master Thesis, Bandung, Indonesia: Institut Teknologi Bandung, 2014.
[21] Jijai, S., Srisuwan, G., O-thong, S., Ismail, N. & Siripatana, C., *Effect of Granule Sizes in the Performance of Upflow Anaerobic Sludge Blanket (UASB) Reactor for Cassava Wastewater Treatment*, Energy Procedia, **79**, pp. 90-97, 2015.
[22] Shete, B. & Shinkar, N., *Kinetic Modeling for Anaerobic Digestion: A Review*, Journal Impact Factor, **5**(2), pp. 127-136, 2014.
[23] Pandian, M., Ngo, H. & Pazhaniappan, S., *Substrate Removal Kinetics of an Anaerobic Hybrid Reactor Treating Pharmaceutical Wastewater,* Journal of Water Sustainability, **1**(3), pp. 301-312, 2011.
[24] Grau, P., Dohanyos, M. & Chudoba, J., *Kinetics of Multicomponent Substrate Removal by Activated Sludge*, Water Research, **9**, pp. 637-642, 1975.
[25] Winkler, M., *Segregation of Biomass in Aerobic Granular Sludge*, Delft: Technnische Universiteit Delft, 2012.
[26] Tay, J., Yang, S. & Liu, Y., *Hydraulic Selection Pressure-induced Nitrifying Granulation in Sequencing Batch Reactor*, Appl Microbiol Biotechnol, **59**, pp. 332-337, 2002.
[27] Wan, C., Yang, X., Lee, D., Sun, S., Liu, X. & Zhang, P., *Influence of Hydraulic Retention Time on Partial Nitrification of Continuous-Flow Aerobic Granular-Sludge Reactor*, Environmental Technology, **35**(14), pp. 1760-1765, 2014.
[28] Val del Rio, A., Figueroa, M., Mosquera-Corral, A., Campos, J. & Mendez, R., *Stability of Aerobic Granular Biomass Treating the Effluent from a Seafood Industry,* International Journal of Environmental Research, **7**(2), pp. 265-276, 2013.
[29] Zheng, Y.M., Yu, H.Q., Liu, S. J. & Liu, X.Z., *Formation and Instability of Aerobic Granules under High Organic Loading Conditions*, Chemosphere, **63**(19), pp. 1791-1800, 2006.
[30] Sponza, D., *Investigation of Extracellular Polymer Substances (EPS) and Physicochemical Properties of Different Activated Sludge Flocs under Steady State Conditions*, Enzyme and Microbial Technology, **32**, pp. 375-385, 2003.
[31] Sponza, D., *Kinetic of Carbonaceous Substrate in an Upflow Anaerobic Sludge Blanket (UASB) Reactor Treating 2,4 Dichlorophenol (2,4 DCP)*, Journal of Environmental Management, **86**, pp. 121-131, 2008.